Macromolecules
ARTICLE

Macromolecules **2010**, *43*, 8063–8070 **8063**
DOI: 10.1021/ma101709h

Synthesis and Electronic Properties of Semiconducting Polymers Containing Benzodithiophene with Alkyl Phenylethynyl Substituents

Prakash Sista,[†] Hien Nguyen,[†] John W. Murphy,[†] Jing Hao,[†] Daniel K. Dei,[†] Kumaranand Palaniappan,[†] John Servello,[†] Ruvini S. Kularatne,[†] Bruce E. Gnade,[†] Bofei Xue,[‡] Paul C. Dastoor,[‡] Michael C. Biewer,[†] and Mihaela C. Stefan*,[†]

[†]*Departments of Chemistry and Materials Science and Engineering, University of Texas at Dallas, 800 West Campbell Road, Richardson, Texas 75080, and* [‡]*Centre for Organic Electronics, The University of Newcastle, University Drive, Callaghan NSW 2308, Australia*

Received July 28, 2010; Revised Manuscript Received September 7, 2010

ABSTRACT: Semiconducting polymers containing benzodithiophene with decyl phenylethynyl and hexadecyl phenylethynyl substituents have been synthesized by Stille coupling polymerization. The optoelectronic properties of the synthesized polymers have been investigated. The synthesized polymers were tested in bulk heterojunction solar cells.

Introduction

The field of organic electronics is based on the development of organic semiconducting materials as a low-cost alternative to traditional inorganic electronic materials.[1] Conjugated organic molecules, oligomers, and polymers are currently used as semiconducting materials in organic field-effect transistors (OFET),[2] organic light-emitting diodes (OLED),[3] solar cells,[4−6] sensors, and organic circuits for integration in low-cost large-area electronics.[7] Currently, most studies of organic semiconductors focus on solution processable semiconducting polymers due to their advantages over conventional inorganic electronic semiconductors in terms of facile deposition, large coverage area, and flexibility.[1] While poly(3-hexylthiophene) is still at the forefront of organic electronics research, the number of new semiconducting polymers with improved electronic properties is increasing rapidly.[8] Chemical modification of thiophene cores and synthesis of fused-ring thiophene derivatives are two of the most common synthetic strategies to generate novel semiconducting polymers with improved optoelectronic properties.[8] In order to maintain the electronic and photonic benefits of regioregular poly(3-hexylthiophene), but still allow control of the molecular orbital levels for the polymer, the fused benzodithiophene monomer core has been studied.[9−27] The fused central ring allows the incorporation of substituents on the central benzene core, while also maintaining planarity of the two thiophene units. In addition, the symmetric nature of the benzodithiophene core eliminates any potential regioirregularity during the polymerization process.

Previously groups have attached electron-donating alkyl and alkoxy substituents on the central benzene ring.[28] In order to create polymers with a better molecular orbital overlap for molecular electronic devices, however, we targeted the synthesis of monomers with greater electron delocalization to generate polymers with a lower band gap. The substitution of two phenylethynyl groups on the central fused benzene ring allows extended electron delocalization. We have recently published the synthesis of benzodithiophene monomers with phenylethynyl substituents and the polymerization of the monomer, along with alternating copolymers with fluorene and carbazole cores.[29] Benzodithiophene monomers with phenylethynyl substituents have aromatic conjugation in two perpendicular directions. The benzodithiophene core along one direction can be used to create a semiconducting thiophene based polymer through typical polymerization techniques. The perpendicular direction, however, has three aromatic units separated by conjugating alkyne units. The bis(phenylethynyl)aromatic conjugation direction can be used as a handle to control the supramolecular alignment of the aromatic units. By having this control, a better conjugation of the π orbitals of the aromatic units can be obtained, and thus better optoelectronic properties can be achieved.[30−32]

In this paper, we present the synthesis and characterization of novel polymers containing benzodithiophene with phenylethynyl substituents containing more soluble longer decyl and hexadecyl alkyl chains, and we demonstrate that these new polymers show promise as active layer components in bulk heterojunction organic photovoltaic devices.

Experimental Section

Materials. All commercial chemicals were purchased from Aldrich Chemical Co., Inc., and were used without further purification unless otherwise noted. All reactions were conducted under purified nitrogen. The polymerization glassware and syringes were dried at 120 °C for at least 24 h before use and cooled under a nitrogen atmosphere. Tetrahydrofuran was dried over sodium/benzophenone ketyl and freshly distilled prior to use. 4,8-Dihydrobenzo[1,2-*b*:4,5-*b*′]dithiophen-4,8-dione was prepared according to the literature.[33]

Synthesis of 4-Decanoyl-1-bromobenzene. Decanoyl chloride (6.55 g, 0.0344 mol) was added dropwise to a solution of bromobenzene (11.39 g, 0.0725 mol) and aluminum chloride (5.17 g, 0.0389 mol). The reaction mixture was heated at 60 °C for 1 h, cooled by pouring it into 300 mL of ice water, and extracted with methylene chloride. The organic layer was washed with 200 mL of 2 N HCl and 200 mL of brine, dried with magnesium sulfate, and concentrated to yield a white solid which was purified by recrystallization form hexane to obtain 6.11 g of solid (0.0196 mol, 57%). ^{1}H NMR ($CDCl_3$, 400 MHz) δ: 0.86 (t, 3H), 1.25 (m, 12H), 1.72 (m, 2H), 2.9 (t, 2H), 7.58 (m, 1H), 7.81 (d, 2H).

*Corresponding author. E-mail: mci071000@utdallas.edu.

Published on Web 09/16/2010

Synthesis of 4-Decyl-1-bromobenzene. 4-Decanoyl-1-bromobenzene (14.20 g, 0.0457 mol), hydrazine monohydrate (12 mL, 0.160 mol), and potassium hydroxide (18.80 g, 0.336 mol) were diluted in 14 mL of 1-octanol. Solution was heated at reflux for 3 h. After cooling to room temperature, the mixture was diluted with ether (200 mL), washed with 2 N HCl (200 mL), washed with brine (200 mL), dried with magnesium sulfate, filtered, and concentrated to yield a yellow oil which was purified by column chromatography (hexane eluent) to yield 8.607 g of clear oil (0.0290 mol, 64%). ^{1}H NMR ($CDCl_3$, 400 MHz) δ: 0.87 (t, 3H), 1.25 (m, 14H), 1.56 (m, 2H), 2.54 (t, 2H), 7.03 (d, 2H), 7.37 (d, 2H).

Synthesis of 4-Decyl-1-trimethylsilylethynylbenzene. 4-Decyl-1-bromobenzene (5.50 g, 0.0185 mol), 0.050 g of copper iodide, and 0.605 g of bistriphenylphosphine dichloropalladium(II) was diluted with 25 mL of triethylamine under nitrogen before adding trimethylsilylacetylene (2.80 mL, 0.0201 mol) at 50 °C. After addition, solution was heated at 80 °C for 24 h before reaction was quenched with 2 N HCl solution (200 mL), extracted with ether (200 mL), washed with brine (200 mL), dried with magnesium sulfate, filtered, and concentrated to yield a brown oil which was purified by column chromatography (hexane eluent) to obtain 4.36 g of clear oil (0.0139 mol, 75%). ^{1}H NMR ($CDCl_3$, 400 MHz) δ: 0.24 (s, 9H), 0.88 (t, 2H), 1.26 (m, 14H), 1.58 (m, 2H), 2.58 (t, 2H), 7.09 (d, 2H), 7.37 (d, 2H).

Synthesis of 4-Decyl-1-ethynylbenzene. 4-Decyl-1-trimethylsilylethynylbenzene (1.99 g, 0.006 34 mol) was diluted with 30 mL of CH_2Cl_2, to which a solution of 2 g of potassium hydroxide dissolved in 30 mL of methanol was added. The mixture was stirred at room temperature for 1 h before being diluted with water (200 mL) and extracted with CH_2Cl_2 (200 mL), dried with magnesium sulfate, filtered, and concentrated to yield a clear oil which was purified by column (hexane) to obtain 1.53 g of oil (0.006 32 mol, 99%). ^{1}H NMR ($CDCl_3$, 400 MHz) δ: 0.87 (t, 3H), 1.26 (m, 14H), 1.57 (m, 2H), 2.59 (t, 2H), 3.02 (s, 1H), 7.12 (d, 2H), 7.39 (d, 2H).

Synthesis of 4,8-Bis(4-decylphenylethynyl)benzo[1,2-*b*:4,5-*b*′]dithiophene. 4-Decyl-1-ethynylbenzene (1.50 g, 0.006 20 mol) was dissolved in 30 mL of dry THF. At 0 °C, 2.5 mL of 2.5 M *n*-BuLi in hexane (0.006 25 mol) was added dropwise to the solution of 4-decyl-1-ethynylbenzene. The reaction mixture was stirred for 30 min at 0 °C followed by the addition of 4,8-dihydrobenzo[1,2-*b*:4,5-*b*′]dithiophen-4,8-dione (0.650 g, 0.002 95 mol) dissolved in 50 mL of THF. After addition, the reaction mixture was heated at reflux for 1 h. At 0 °C, 3.85 g of tin chloride dihydrate dissolved in 50 mL of 20% HCl solution was added, and then the reaction was heated at reflux for 2 h. The reaction was diluted with ether (200 mL), and the organic layer was washed with water (2 × 200 mL), dried with magnesium sulfate, filtered, and concentrated to 10 mL of reddish solution which was added to 200 mL of methanol, upon which a yellow solid precipitated out of solution. The yellow solid was filtered to obtain 1.033 g of product (0.001 54 mol, 52%). ^{1}H NMR ($CDCl_3$, 400 MHz) δ: 0.88 (t, 6H), 1.27 (m, 28H), 1.64 (m, 4H), 2.66 (t, 4H), 7.22 (d, 4H), 7.57 (d, 2H), 7.59 (d, 2H), 7.7 (d, 2H). ^{13}C NMR ($CDCl_3$, 100 MHz) δ: 14.1, 22.7, 29.28, 29.34, 29.5, 29.6, 29.63, 31.3, 31.9, 36.0, 85.1, 99.5, 112.09, 120.0, 123.3, 128.0, 128.6, 131.7, 138.2, 140.3, 144.8. Anal. calculated for $C_{46}H_{54}S_2$: C, 82.33%; H, 8.11%. Found: C, 81.4%; H, 8.21%.

Synthesis of 2,6-Dibromo-4,8-bis(4-decylphenylethynyl)benzo-[1,2-*b*:4,5-*b*′]dithiophene. 4,8-Bis(4-decylphenylethynyl)benzo-[1,2-*b*:4,5-*b*′]dithiophene (0.404 g, 0.000 603 mol) was dissolved in 100 mL of dry THF and cooled to −78 °C. 0.85 mL of 1.6 M *n*-BuLi in hexane (0.001 36 mol, 2.2 equiv) was added, and the solution was stirred for 1 h at −78 °C. After *n*-BuLi addition the solution turned to a fluorescent green color. Carbon tetrabromide (0.477 g) dissolved in 20 mL of THF was added. After stirring for 15 min at −78 °C, the solution was allowed to warm to room temperature for 1 h. Solvent was removed, and the brown solid was dissolved in chloroform and washed with water (2 × 200 mL), dried with magnesium sulfate, filtered, and concentrated to obtain a thick oil, which was poured into 200 mL of methanol. The yellow solid that precipitated was filtered to obtain 0.375 g of product (0.000 453 mol, 75%). ^{1}H NMR ($CDCl_3$, 400 MHz) δ: 0.88 (t, 6H), 1.28 (m, 28H), 1.64 (m, 4H), 2.66 (t, 4H), 7.23 (d, 4H), 7.55 (d, 4H), 7.64 (s, 2H). ^{13}C NMR ($CDCl_3$, 100 MHz) δ: 14.1, 22.7, 29.28, 29.34, 29.5, 29.6, 29.63, 31.3, 31.9, 36.0, 84.1, 100.3, 110.2, 117.2, 119.5, 126.0, 128.7, 131.7, 137.3, 141.2, 144.5. Anal. calculated for $C_{46}H_{52}Br_2S_2$: C, 66.66%; H, 6.32%. Found: C, 65.93%; H, 6.13%.

Synthesis of 2,6-(Trimethyltin)-4,8-bis(4-decylphenylethynyl)-benzo[1,2-*b*:4,5-*b*′]dithiophene. 4,8-Bis(4-decylphenylethynyl)-benzo[1,2-*b*:4,5-*b*′]dithiophene (0.272 g, 0.000 406 mol) was dissolved in 100 mL of dry THF. Under nitrogen at −78 °C, 0.60 mL of 1.6 M *n*-BuLi in hexane was added (0.000 96 mol, 2.3 equiv). The solution turned to a fluorescent green color upon addition. Reaction was stirred at −78 °C for 1 h before 0.90 mL of 1 M trimethyltin chloride was added. Reaction was stirred at −78 °C for 30 min before allowing to warm to room temperature. Solvent was evaporated, and the yellow solid was dissolved in chloroform and solution was washed with water (2 × 200 mL), dried with magnesium sulfate, filtered, and concentrated. The solid was dissolved in 10 mL of THF and added to 200 mL of methanol. The yellow solid was filtered to obtain 0.346 g of product (0.000 348 mol, 86%). ^{1}H NMR ($CDCl_3$, 400 MHz) δ: 0.47 (s, 18 H) 0.89 (t, 6H), 1.27 (m, 28H), 1.62 (m, 4H), 2.66 (t, 4H), 7.23 (d, 4H), 7.61 (d, 4H), 7.73 (s, 2H). ^{13}C NMR ($CDCl_3$, 100 MHz) δ: −8.3, 14.1, 22.7, 29.27, 29.34, 29.5, 29.6, 29.7, 31.3, 31.9, 36.0, 85.7, 98.8, 110.2, 120.3, 128.5, 130.9, 131.7, 138.9, 143.4, 143.9, 144.6. Anal. calculated for $C_{52}H_{70}S_2Sn_2$: C, 62.66%; H, 7.08%. Found: C, 62.33%; H, 7.08%.

Synthesis of Poly{4,8-bis(4-decylphenylethynyl)benzo[1,2-*b*:4,5-*b*′]dithiophene} (P1). To a three-neck round-bottom flask were added 2,6-dibromo-4,8-bis(4-decylphenylethynyl)benzo-[1,2-*b*:4,5-*b*′]dithiophene (1.17 g, 1.413 mmol), 2,6-(trimethyltin)-4,8-bis(4-decylphenylethynyl)benzo[1,2-*b*:4,5-*b*′]dithiophene (1.49 g, 1.5 mmol), and tetrakis(triphenylphosphine)palladium(0) (0.08 g, 0.07 mmol) under a nitrogen atmosphere. Toluene (60 mL) and DMF (2 mL) were added to dissolve the monomers. The solution was heated at reflux for 2 h, at which time 20 mL of toluene was added to the reaction mixture. After an additional 3 h at reflux, 40 mL of toluene was added to the reaction mixture. The polymerization was stopped after 48 h by precipitating the polymer in methanol. The polymer was filtered, and the polymer was purified by Soxhlet extractions with methanol, diethyl ether, hexane, dichloromethane, and chloroform. The polymer was obtained from the chloroform fraction upon evaporation of solvent. The polymer was obtained as a dark red solid (1.3 g, 70% yield). ^{1}H NMR (toluene-d_8, 400 MHz) δ: 0.42 (s, 18H), 0.95 (t, 6H), 1.25 (br, 56H), 2.7 (br, 4H), 7.2 (br, 8H), 7.55 (br, 2H).

4-Hexadecanoyl-1-bromobenzene was synthesized as 4-decanoyl-1-bromobenzene using hexadecanoyl chloride. ^{1}H NMR ($CDCl_3$, 400 MHz) δ: 0.86 (t, 3H), 1.24 (m, 26H), 1.7 (m, 2H), 2.9 (t, 2H), 7.6 (d, 2H), 7.8 (d, 2H).

4-Hexadecyl-1-bromobenzene was synthesized as 4-decyl-1-bromobenzene. ^{1}H NMR ($CDCl_3$, 400 MHz) δ: 0.87 (t, 3H), 1.26 (m, 26H), 1.57 (m, 2H), 2.55 (t, 2H), 7.04 (d, 2H), 7.37 (d, 2H).

4-Hexadecyl-1-trimethylsilylethynylbenzene was synthesized as 4-decyl-1-trimethylsilylethynylbenzene. ^{1}H NMR ($CDCl_3$, 400 MHz) δ: 0.22 (s, 9H), 0.87 (t, 2H), 1.27 (m, 26H), 1.54 (m, 2H), 2.56 (t, 2H), 7.08 (d, 2H), 7.35 (d, 2H).

4-Hexadecyl-1-ethynylbenzene was synthesized as 4-decyl-1-ethynylnenzene. ^{1}H NMR ($CDCl_3$, 400 MHz) δ: 0.86 (t, 3H), 1.24 (m, 26H), 1.56 (m, 2H), 2.58 (t, 2H), 3. (s, 1H), 7.09 (d, 2H), 7.39 (d, 2H).

4,8-Bis(4-hexadecylphenylethynyl)benzo[1,2-b:4,5-b′]dithiophene was synthesized as 4,8-bis(4-decylphenylethynyl)benzo[1,2-*b*:4,5-*b*′]dithiophene. ^{1}H NMR ($CDCl_3$, 400 MHz) δ: 0.88

(t, 6H), 1.27 (m, 52H), 1.64 (m, 4H), 2.65 (t, 4H), 7.22 (d, 4H), 7.57 (d, 2H), 7.6 (d,2H), 7.71 (d, 2H). ^{13}C NMR ($CDCl_3$, 100 MHz) δ: 14.0, 22.7, 29.28, 29.38, 29.51, 29.6, 29.68, 29.71, 31.3, 31.9, 36.0, 85.1, 99.5, 112.09, 120.0, 123.3, 128.0, 128.6, 131.7, 138.2, 140.3, 144.2. Anal. calculated for $C_{58}H_{78}S_2$: C, 82.99%; H, 9.37%. Found: C, 82.2%; H, 8.96%.

2,6-Dibromo-4,8-bis(4-hexadecylphenylethynyl)benzo[1,2-b:4,5-b′]-dithiophene was synthesized as 2,6-dibromo-4,8-bis(4-decylphenylethynyl)benzo[1,2-*b*:4,5-*b*′]dithiophene. ^{1}H NMR ($CDCl_3$, 400 MHz) δ: 0.88 (t, 6H), 1.27 (m, 52H), 1.65 (m, 4H), 2.65 (t, 4H), 7.21 (d, 4H), 7.50 (d, 4H), 7.64 (s, 2H). ^{13}C NMR ($CDCl_3$, 100 MHz) δ: 14.1, 22.7, 29.3, 29.4, 29.5, 29.6, 29.71, 29.72, 29.74, 29.75, 31.2, 31.9, 36.1, 84.2, 100.6, 110.5, 117.4, 119.7, 126.2, 128.7, 131.9, 137.6, 141.5, 144.7. Anal. calculated for $C_{58}H_{76}Br_2S_2$: C, 69.86%; H, 7.68%. Found: C, 69.64%; H, 7.38%.

2,6-(Trimethyltin)-4,8-bis(4-hexadedecylphenylethynyl)benzo-[1,2-b:4,5-b′]dithiophene was synthesized as 2,6-(trimethyltin)-4,8-bis(4-dedecylphenylethynyl)benzo[1,2-*b*:4,5-*b*′]dithiophene. ^{1}H NMR ($CDCl_3$, 400 MHz) δ: 0.48 (s, 18 H), 0.89 (t, 6H), 1.29 (m, 52H), 1.6 (m, 4H), 2.65 (t, 4H), 7.22 (d, 4H), 7.61 (d, 4H), 7.73 (s, 2H). ^{13}C NMR ($CDCl_3$, 100 MHz) δ: −8.25, 14.1, 22.7, 29.28, 29.37, 29.52, 29.6, 29.7, 31.26, 31.94, 36.01, 85.7, 98.77, 110.2, 120.3, 128.57, 130.9, 131.7, 138.99, 143.35, 143.9, 144.6. Anal. calculated for $C_{64}H_{94}S_2Sn_2$: C, 65.98%; H, 8.13%. Found: C, 67.0%; H, 8.08%.

Synthesis of Poly{4,8-bis(4-hexadecylphenylethynyl)benzo-[1,2-b:4,5-b′]dithiophene} (**P2**) was synthesized as polymer **P1**. ^{1}H NMR (toluene-d_8, 400 MHz) δ: 0.5 (s, 18H), 0.96 (t, 6H), 1.30 (br, 56H), 2.6 (br, 4H), 7.2 (br, 8H), 7.55 (br, 2H).

Structural Analysis. ^{1}H NMR spectra of the synthesized monomers and polymers were recorded on a Bruker 400 MHz spectrometer at 25 °C. ^{1}H NMR data are reported in parts per million as chemical shift relative to tetramethylsilane (TMS) as the internal standard. Spectra of monomers were recorded in $CDCl_3$. ^{1}H NMR spectra of the polymers were recorded in toluene-d_8 at 55 °C. GC/MS was performed on an Agilent 6890-5973 GC-MS workstation. The GC column was a Hewlett-Packard fused silica capillary column cross-linked with 5% phenylmethylsiloxane. Helium was the carrier gas (1 mL/min). The following conditions were used for all GC/MS analyses: injector and detector temperature, 250 °C; initial temperature, 70 °C; temperature ramp, 10 °C/min; final temperature, 280 °C. The UV−vis spectra of polymer solutions in chloroform solvent were carried out in 1 cm cuvettes using an Agilent 8453 UV−vis spectrometer. Thin films of polymer were obtained by evaporation of chloroform solvent on glass microscope slides. Fluorescence spectra were recorded on a Perkin-Elmer LS 50 BL luminescence spectrometer. Molecular weights of the synthesized polymers were measured by size exclusion chromatography (SEC) analysis on a Viscotek VE 3580 system equipped with ViscoGEL columns (GMHHR-M), connected to a refractive index (RI) detectors. GPC solvent/sample module (GPCmax) was used with HPLC grade THF as the eluent, and calibration was based on polystyrene standards. Running conditions for SEC analysis were flow rate = 1.0 mL/min, injector volume = 100 μL, detector temperature = 30 °C, and column temperature = 35 °C. All the polymers samples were dissolved in THF, and the solutions were filtered through PTFE filters (0.45 μm) prior to injection.

Optoelectronic Properties of the Synthesized Polymers. *Cyclic Voltammetry*. Electrochemical grade tetrabutylammonium perchlorate (TBAP) was used as the electrolyte without further purification. Acetonitrile (low water 99.9% grade) was distilled over calcium hydride (CaH_2). Electrochemical experiments were performed using a BAS CV-50W voltammetric analyzer (Bioanalytical Systems, Inc.). The electrochemical cell was comprised of a platinum electrode, a platinum wire auxiliary electrode, and an Ag/AgCl reference electrode. Acetonitrile solutions containing 0.1 M of tetrabutylammonium perchlorate were placed in a cell and purged with N_2. A drop of the polymer solution in chloroform was placed on tip of the platinum electrode. The solvent was evaporated in air. The film was immersed in the electrochemical cell containing the electrolyte prior to measurements. All electrochemical shifts were standardized to the ferrocene redox couple at 0.471 V.

Preparation of Solar Cell Devices. OLED-grade glass slides were purchased with prepatterned ITO electrodes from Luminescense Technology Corp. (Taiwan.) The coupons were cleaned with deionized water, acetone, and isopropanol successively by sonication for 5 min each and then washed for 10 min in an oxygen plasma prior to use. Immediately following plasma treatment, poly(3,4-ethylenedioxythiophene):poly(styrenesulfonate) (PEDOT:PSS) was spin-coated (3000 min^{-1}, 60 s) followed by annealing at 180 °C for 5 min under nitrogen, resulting in a film thickness of 40 nm. The PCBM/polymer blend was prepared in dichlorobenzene at a 1:1 weight ratio and total concentration of 35 mg/mL. This blend was then spin-cast (600 min^{-1}, 200 min^{-1} s^{-1}, 60 s) onto the PEDOT−PSS/substrate, after which it was immediately placed into a closed Petri dish to finish drying. For the slow evaporation samples a small Petri dish (diameter = 90 mm, height = 13 mm) was used, and drying took ∼60 min; for the fast evaporation a larger Petri dish (diameter = 137 mm, height = 20 mm) was used, and the drying time was about 15 min. Cathodes consisting of aluminum (100 nm) were thermally evaporated at a rate of ∼2.5 Å/s through a shadow mask to define solar cell active areas.

IV testing was carried out under a controlled N_2 atmosphere using a Keithley 236, model 9160 interfaced with LabView software. The solar simulator used was an THERMOORIEL equipped with a 300 W xenon lamp; the intensity of the light was calibrated to 100 mW cm^{-2} with a NREL certified Hamamatsu silicon photodiode. The active area of the devices was 0.1 cm^2. The active layer film thickness was measured using a Veeco Dektak VIII profilometer.

TMAFM (*Tappping Mode Atomic Force Microscopy*). AFM studies were carried out on a VEECO-dimension 5000 scanning probe microscope with a hybrid *xyz* head equipped with NanoScope Software. AFM images were obtained using silicon cantilevers with nominal spring constant of 42 N/m and nominal resonance frequency of 300 kHz (OTESPa). Image analysis software Nanoscope 7.30 was used for surface imaging and image analysis. All AFM measurements were conducted under ambient conditions. All cantilever oscillation amplitude was equal to ca. 375 mV, and all images were acquired at 1 Hz scan frequency. Sample scan area varied from 1 to 5 μm. Samples were prepared from either chloroform or trichlorobenzene solutions (1 mg/mL) via drop-casting onto a mica substrate. The chloroform was slowly evaporated in a cover Petri dish filled with chloroform. The trichlorobenzene was evaporated by heating the mica substrate for 1 h at 60 °C. Samples were annealed at 120 °C for 30 min. For the solar cell devices the AFM images were recorded for spin-cast blends of polymer/PCBM in dichlorobenzene.

Results and Discussion

We have previously reported the synthesis and characterization of polymers containing benzodithiophene with pentylphenylethynyl substituents. Poly{4,8-bis(4-pentylphenylethynyl)benzo-[1,2-*b*:4,5-*b*′]dithiophene} was synthesized by Stille coupling and was found to have relatively low solubility in organic solvents, such as tetrahydrofuran and chloroform.[29] Because of the low solubility, the electronic properties of this polymer could not be investigated. Attachment of longer alkyl substituents to the phenyl ring was expected to increase the solubility of the polymers. In contrast to the commercially available 4-pentylphenylacetylene, the larger alkyl chains needed to be synthesized starting with bromobenzene and attaching an acyl group through a Friedel−Crafts acylation. The decanoyl (C10) and hexadecanoyl (C16) groups were attached in this manner. The carbonyl was reduced by a Wolf−Kishner reaction to generate the para-substituted bromoalkyl derivatives.

Scheme 1. Synthesis of 4,8-Bis(4-alkylphenylethynyl)benzo[1,2-*b*:4,5-*b*′]dithiophene Monomers

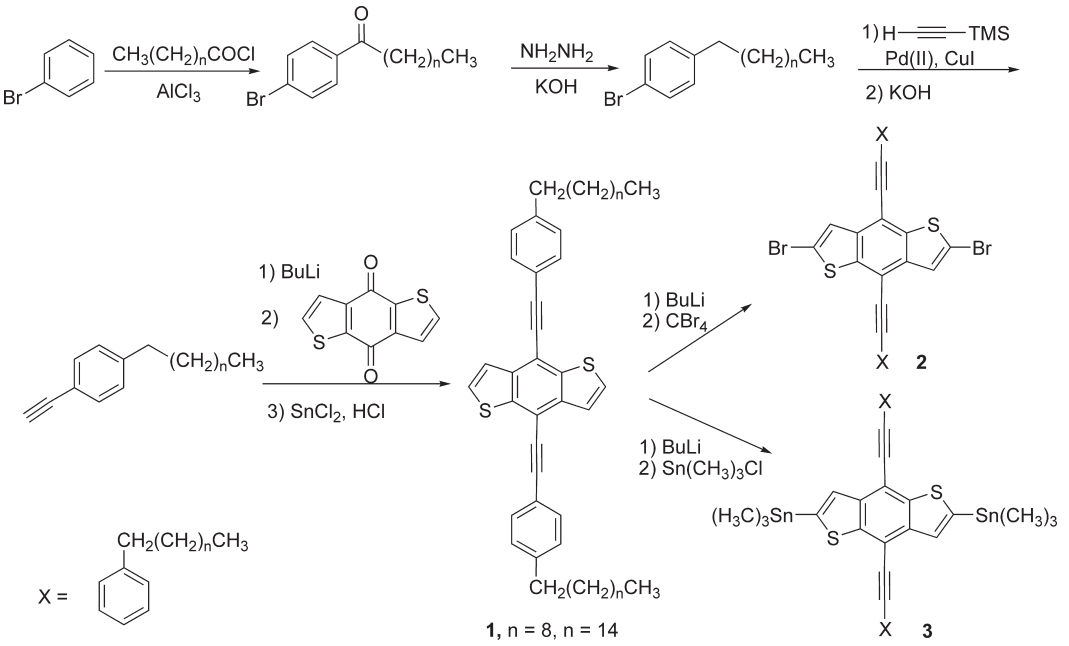

Scheme 2. Synthesis of Poly{4,8-bis(4-decylphenylethynyl)benzo[1,2-*b*:4,5-*b*′]dithiophene} (P1) (*n* = 8) and Poly{4,8-bis(4-hexadecylphenylethynyl)benzo[1,2-*b*:4,5-*b*′]dithiophene} (P2) (*n* = 14)

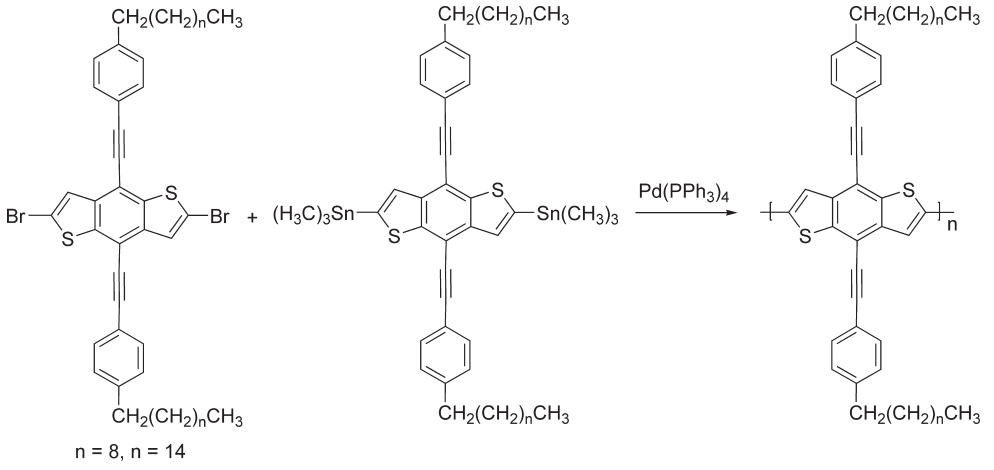

The alkyne group was attached via a Sonogashira coupling with trimethylsilylacetylene (TMS), and the TMS protecting group was subsequently removed in basic conditions to generate the decyl- and hexadecyl-substituted phenylacetylenes, as shown in Scheme 1. These alkynes were reacted with 4,8-dihydrobenzene[1,2-*b*:4,5-*b*′]dithiophen-4,8-dione to generate the benzodithiophene monomers, which were subsequently reacted to form the dibromo and distannylated derivatives, which were used in Stille polymerization to generate poly{4,8-bis(4-decylphenylethynyl)benzo[1,2-*b*:4,5-*b*′]-dithiophene} (**P1**) and poly{4,8-bis(4-hexadecylphenylethynyl)-benzo[1,2-*b*:4,5-*b*′]dithiophene} (**P2**), as shown in Scheme 2.

The number-average molecular weights for both **P1** (23 400 g/mol) and **P2** (27 420 g/mol) are appreciably larger than the previously synthesized poly{4,8-bis(4-pentylphenylethynyl)benzo-[1,2-*b*:4,5-*b*′]dithiophene}(**P3**) (1700 g/mol)[29] due to the higher solubility during polymerization reactions (Table 1). Polymers **P1** and **P2** are soluble in chloroform, tetrahydrofuran, and chlorobenzenes. ^{1}H NMR analysis of polymers in $CDCl_3$ proved to be difficult as the polymers aggregate in solution, resulting in broad features. In order to avoid this drawback, the ^{1}H NMR spectra of polymers were recorded in deuterated toluene at 60 °C (Supporting Information).

The HOMO and LUMO energy levels of polymers **P1** and **P2** were estimated by cyclic voltammetry. From the value of onset oxidation potential and onset reduction potential of polymers **P1** and **P2**, the HOMO, LUMO, and the band gap were calculated (Table 1 and Supporting Information). Both **P1** and **P2** polymers have reversible oxidation and reduction peaks. The HOMO and LUMO energy levels for polymers **P1** and **P2** are very similar, as expected based on their structural similarity. The length of the alkyl substituent does not significantly influence the HOMO and LUMO energy levels, as seen from the results presented in Table 1. The HOMO energy level of polymers **P1** and **P2** (−5.62 and −5.61 eV) is below the air oxidation threshold (ca. −5.27 eV), indicating a good air stability of the synthesized polymers. The band gaps of polymers **P1** and **P2** are lower than our previously reported benzodithiophene polymer with pentyl phenylethynyl substituents (**P3**), which is due to the larger molecular weights, which in turn render a longer conjugation length.

Table 1. Molecular Weights as Well as Optical and Electronic Energy Levels of Poly{4,8-bis(4-decylphenylethynyl)benzo[1,2-*b*:4,5-*b*′]dithiophene} (P1), Poly{4,8-bis(4-hexadecylphenylethynyl)benzo[1,2-*b*:4,5-*b*′]dithiophene} (P2), and Poly{4,8-bis-(4-pentylphenylethynyl)benzo[1,2-*b*:4,5-*b*′]dithiophene} (P3)[29]

polymer	M_n (g/mol)	PDI	λ_{maxL} (nm)	λ_{maxS} (nm)	E_{ox} (V)	E_{red} (V)	HOMO[a] (eV)	LUMO[b] (eV)	E_g (eV)
P1	23 400	3.0	520	525	0.91	−0.81	−5.62	−3.90	1.72
P2	27 420	2.0	520	525	0.90	−0.84	−5.61	−3.87	1.74
P3	1 700	1.9	517	506	0.71	−1.33	−5.42	−3.38	2.04

[a] Estimated from onset oxidation wave. [b] Estimated from onset reduction wave.

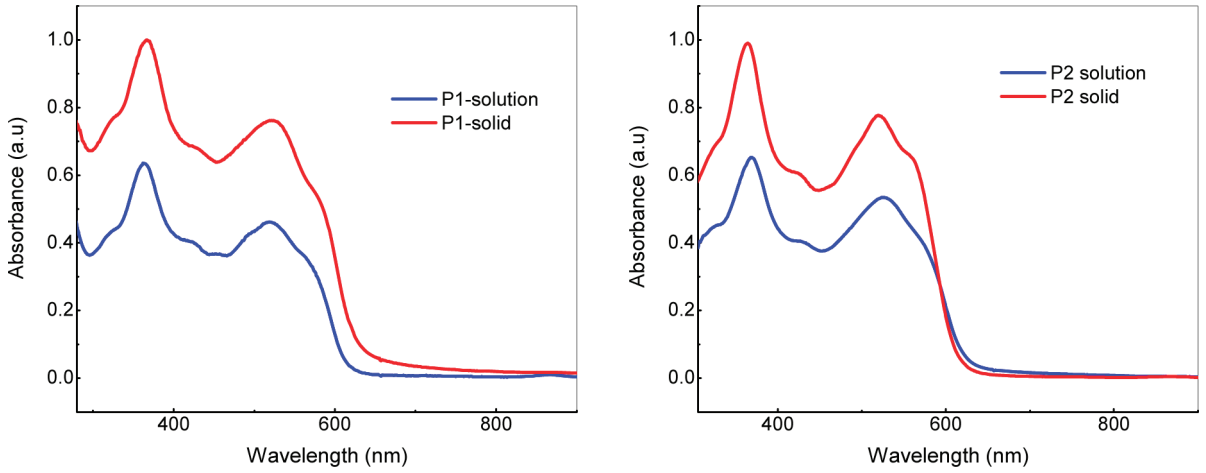

Figure 1. UV−vis absorption spectra of poly{4,8-bis(4-decylphenylethynyl)benzo[1,2-*b*:4,5-*b*′]dithiophene} (**P1**) and poly{4,8-bis(4-hexadecylphenylethynyl)-benzo[1,2-*b*:4,5-*b*′]dithiophene}(**P2**) in chloroform solutions and as thin films drop-cast from chloroform solution.

The UV−vis spectra of the polymers **P1** and **P2** in chloroform solution and films are shown in Figure 1. **P1** and **P2** polymers have similar electronic absorption spectra in chloroform solution, displaying two absorption maxima, at ∼363 and ∼520 nm. The absorption band in the visible region (∼520 nm) is due to the $\pi-\pi^*$ transition of the benzodithiophene backbone, while the band in the UV region (∼363 nm) originates from the 1,4-bis-(phenylethynyl)benzene substituents.[34,35] The intensity of both benzodithiophene and (phenylethynyl)benzene bands correlates with their relative ratio in the repeating unit. The UV−vis absorption spectra in chloroform show a vibronic peak at 570 nm for **P1** and 566 nm for **P2**. A particular feature of the absorption spectra of polymers **P1** and **P2** is the relatively small red shift observed for the UV−vis spectra of films vs chloroform solutions. The absorption bands shifted from 363 nm (in solution) to 366 nm (in film) and from 520 nm (in solution) to 525 nm (in film) for polymer **P1**, while polymer **P2** displayed a shift from 363 nm (in solution) to 366 nm (in film) and from 520 nm (in solution) to 525 nm (in film). Both the presence of the vibronic peak in the solution spectra and the small shift of the absorption maxima from solution to films indicate that the polymers have a rigid rod conformation in the solution and solid state.[25,36]

Fluorescence spectra of polymers **P1** and **P2** have been recorded (Table 2 and Supporting Information). Polymer **P1** displays emission at 526 nm, while polymer **P2** displays emission at 519 nm, upon excitation at 355 nm. The fluorescence quantum yields for polymers **P1** and **P2** have been calculated by using rhodamine B as standard. The quantum yields of the three polymers **P1**, **P2**, and **P3** are 18.8%, 14.5%, and 48%, respectively.

The morphology of polymers **P1** and **P2** was investigated by TMAFM. Films were deposited by drop-casting from chloroform and trichlorobenzene solutions onto mica substrates. Films deposited from chloroform solution for polymers **P1** and **P2** display granular morphology as shown in Figure 2 and the Supporting Information. However, the film of polymer **P1**

Table 2. Fluorescence Data for Poly{4,8-bis-(4-decylphenylethynyl)benzo[1,2-*b*:4,5-*b*′]dithiophene} (P1), Poly-{4,8-bis(4-hexadecylphenylethynyl)benzo[1,2-*b*:4,5-*b*′]dithiophene} (P2), and Poly{4,8-bis(4-pentylphenylethynyl)benzo-[1,2-*b*:4,5-*b*′]dithiophene} (P3)[29]

polymer[a]	excitation (nm)	emission (nm)	quantum yield (%)
P1	355	526	18.8
P2	355	519	14.5
P3	400	505	48.0

[a] Fluorescence was measured in chloroform solution.

deposited from trichlorobenzene followed by the evaporation of solvent at 60 °C displays different morphological features as compared to films deposited from chloroform. Figure 2 shows the TMAFM phase and height images for thin films of polymer **P1** deposited from both chloroform and trichlorobenzene solutions. The 3D AFM images displayed in Figure 3 show that the polymer film deposited from trichlorobenzene solution forms rounded grains, which result in a nonuniform film surface. A possible explanation for the presence of the rounded grains could be the development of a columnar morphology, which cannot be proved by using TMAFM imaging. Further insight into the morphology of these polymers is currently under investigation by using cross-section TEM measurements on films deposited from various high boiling point solvents.

The photovoltaic properties of polymers **P1** and **P2** were investigated in bulk heterojunction solar cells with [6,6]-phenyl-C61-butyric acid methyl ester (PCBM). The solar cells were fabricated using a conventional device structure: ITO/PEDOT:PSS/P:PCBM/Al. The PCBM/polymer blend was prepared in dichlorobenzene at 1:1 weight ratio. This blend was spin-cast onto the substrate, after which it was placed into a closed Petri dish to finish drying. Slow and fast evaporation samples were obtained. The approximate drying time for the fast evaporation was 15 min, while for the slow evaporation the drying time was 60 min. The $I-V$ curves (Figure 4) for both polymers **P1** and **P2** are shown in Figure 4, and Table 3 lists the photovoltaic properties obtained from the $I-V$ curves. As listed in Table 3, the power

conversion efficiencies (PCE) of devices prepared with polymer **P2** are 50% lower as compared to polymer **P1**.

Thus, the solar cell device performance appears to depend upon the ratio between the insulating alkyl substituents and the semiconducting benzodithiophene backbone, with polymer **P2** with hexadecyl substituents having lower performance as compared to polymer **P1** with decyl substituents. In addition, the field-effect mobility measured in bottom-gate bottom-contact transistors of polymer **P2** ($\mu = 1 \times 10^{-6}$ cm^2 V^{-1} s^{-1}) is 2 orders of magnitude lower as compared to polymer **P1** ($\mu = 1.6 \times 10^{-4}$ cm^2 V^{-1} s^{-1}). The results presented in Figure 4 and Table 3 also show that devices fabricated by slow evaporation have higher PCE than those fabricated by fast evaporation. For example, polymer **P1** has a PCE of ~0.5% in devices obtained by fast evaporation, while devices obtained by slow evaporation have a PCE of ~1.05%. This trend is consistent for polymer **P2**, which showed a power conversion efficiency of ~0.25% in the fast evaporation device, while a PCE of ~0.47% was obtained for the slow evaporation device. A comparison of the TMAFM images of the fast and slow evaporated **P1**/PCBM and **P2**/PCBM binary blend devices reveals that, for both systems, the morphology of the fast evaporated surfaces are rougher than the slow evaporated surfaces and show more evidence of phase-segregated features (Figure 5 and Supporting Information). We speculate that, similar to the well-studied P3HT/PCBM system, these features are associated with the phase segregation of PCBM islands during fast evaporation process.[37,38] Interestingly, this structure–function relationship is opposite to that observed P3HT/PCBM solar cells, where slowly evaporated films produce rougher surfaces and consequently better performing solar cell devices.[39,40] Moreover, this phase segregation is more marked in **P2**/PCBM blends compared with the **P1**/PCBM blend surfaces. It seems reasonable to hypothesize, therefore, that the lower solar cell performance of the **P2**/PCBM devices relative to the **P1**/PCBM devices (together with the observed dependence of PCE upon

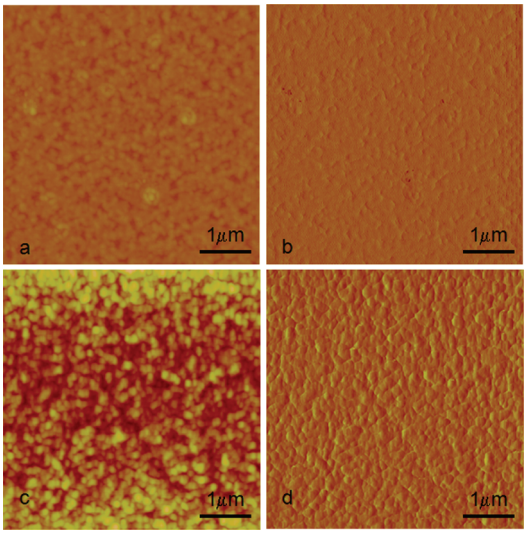

Figure 2. TMAFM phase (right) and height (left) images of poly{4,8-bis(4-decylphenylethynyl)benzo[1,2-*b*:4,5-*b*′]dithiophene} (**P1**): (a, b) films deposited by drop-casting from chloroform solution; (c, d) films deposited by drop-casting from trichlorobenzene solution. Scan size: 5 × 5 μm.

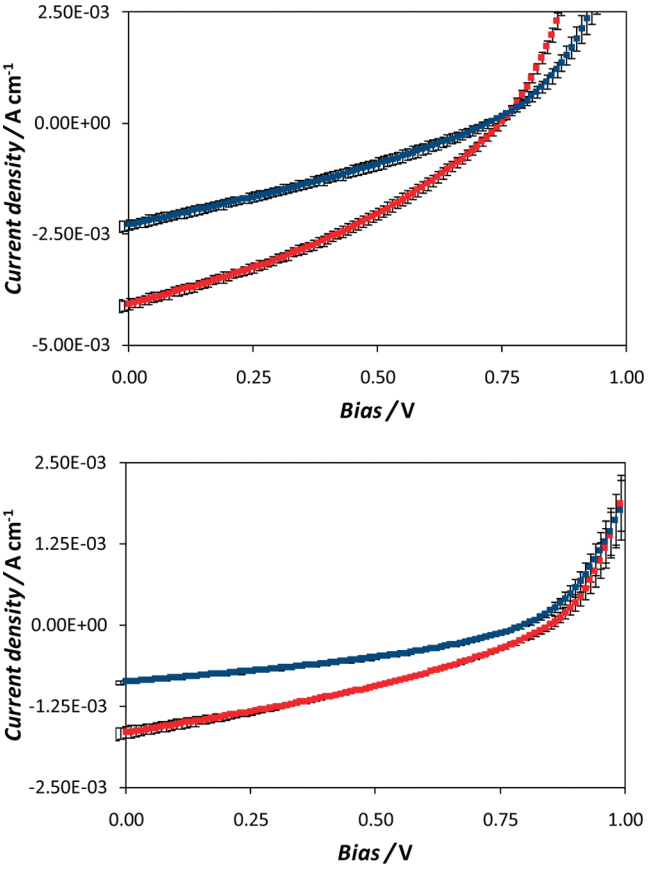

Figure 4. *I*–*V* plots for the polymer solar cells based on **P1** (top) and **P2** (bottom). [P1]:[PCBM] = 1:1 (w/w); [P2]:[PCBM] = 1:1 (w/w); the blue curves represent devices obtained by fast evaporation, and the red curves represent devices obtained by slow evaporation. The error bars represent the standard deviation from the average for the working devices on a coupon.

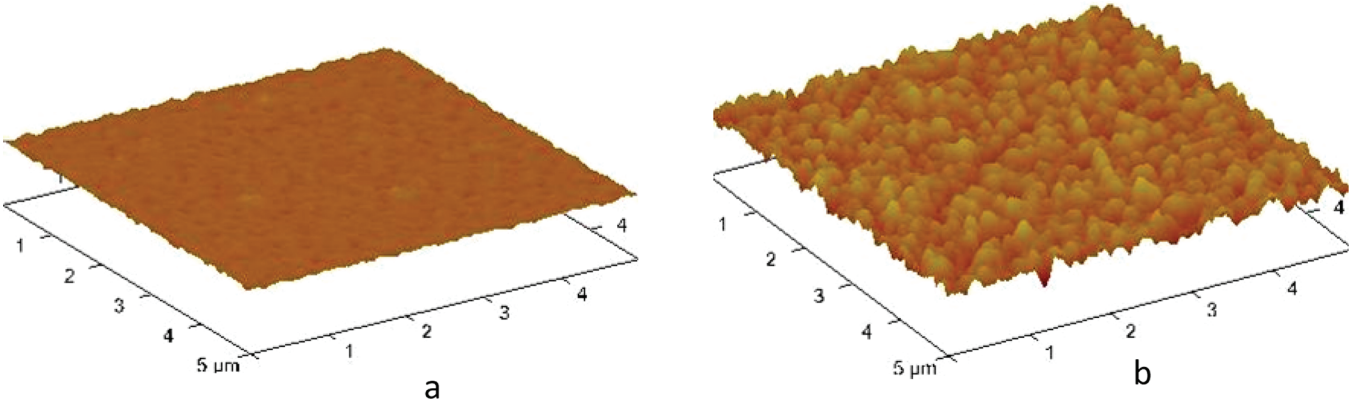

Figure 3. 3D height TMAFM images of thin films of polymer **P1**: (a) film deposited by drop-casting from chloroform solution; (b) film deposited by drop-casting from trichlorobenzene.

Table 3. Photovoltaic Properties of Poly{4,8-bis(4-decylphenylethynyl)benzo[1,2-*b*:4,5-*b*′]dithiophene} (P1) and Poly{4,8-bis(4-hexadecylphenylethynyl)benzo[1,2-*b*:4,5-*b*′]dithiophene} (P2)[a]

polymer	evaporation	active layer thickness (nm)	V_{OC} (V)	ISC (mA/cm^2)	FF	η (%)
P1	slow	280	0.75	4.0	0.34	1.05
P1	fast	250	0.73	2.0	0.30	0.50
P2	slow	170	0.85	3.3	0.33	0.47
P2	fast	190	0.80	0.87	0.35	0.25

[a] Spin-coated films of polymer/PCBM (1:1 w:w).

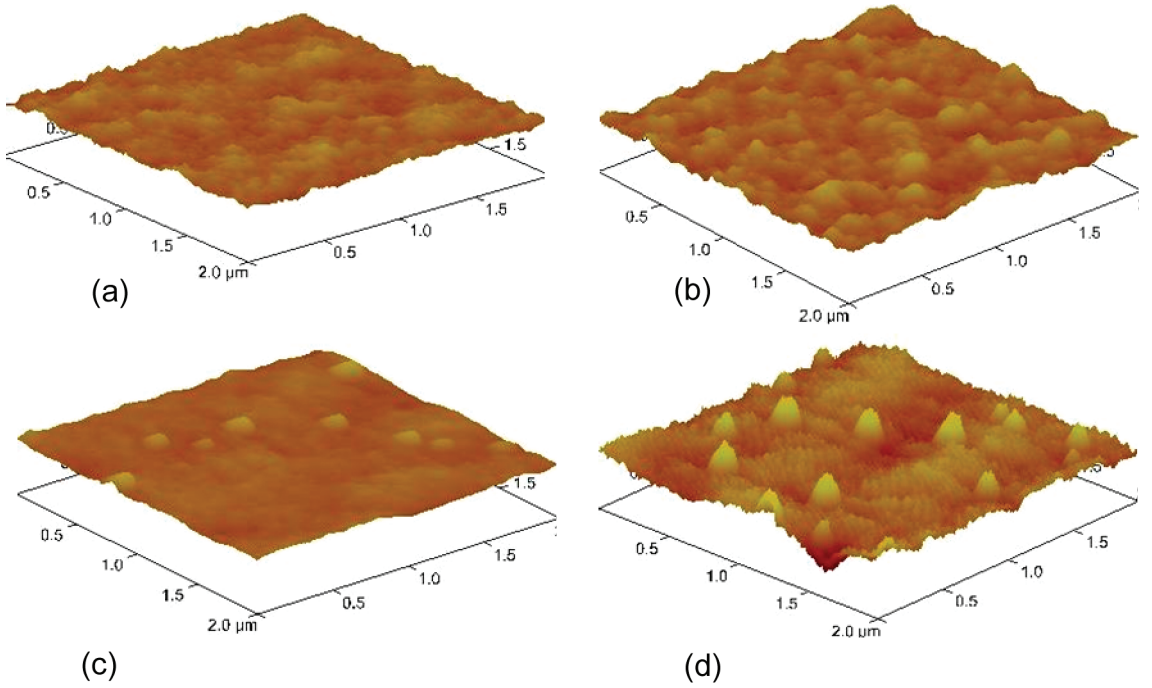

Figure 5. 3D TMAFM phase images of solar cell devices: (a) **P1**/PCBM active layer (slow evaporation); (b) **P1**/PCBM active layer (fast evaporation); (c) **P2**/PCBM active layer (slow evaporation); (d) **P2**/PCBM active layer (fast evaporation).

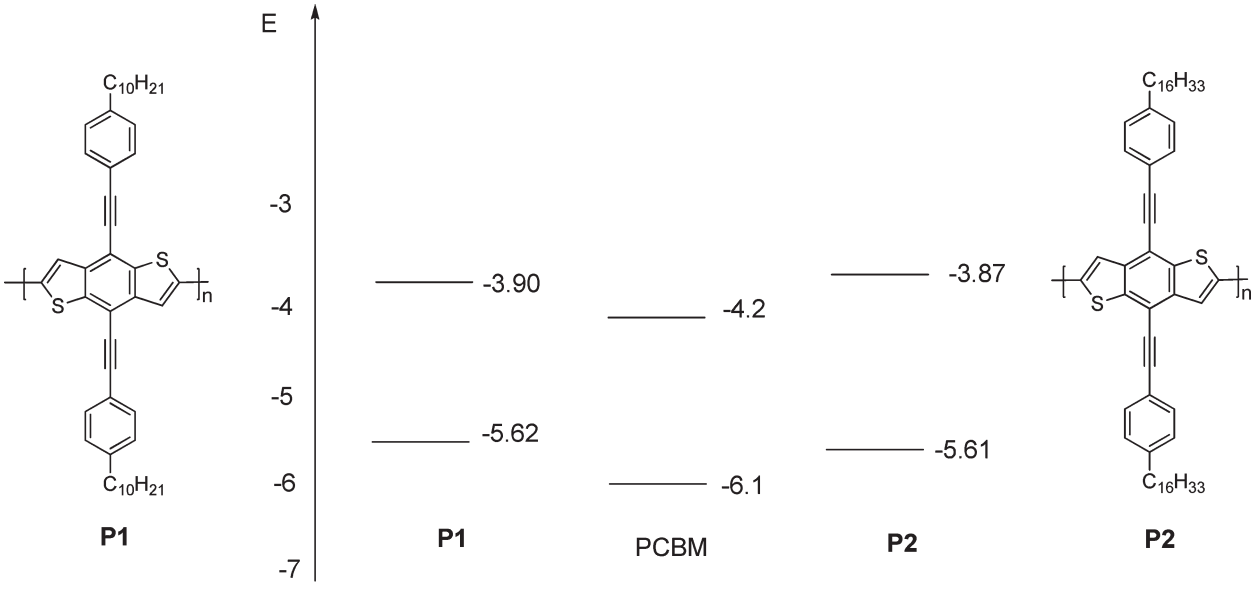

Figure 6. **P1**, **P2** donors and PCBM acceptor energy levels.

evaporation rate) arises from the observed differences in morphology resulting in lower J_{sc} currents.

All the solar cell devices have relatively high open circuit voltage (V_{OC}) which is due to the relatively low HOMO energy levels of polymers **P1** and **P2** (−5.62 and −5.61 eV). However, the measured V_{OC} (0.7−0.85 V) are lower than the theoretical predicted values (1.12 and 1.11 eV),[41] which is most likely attributed to charge carrier recombination losses at the polymer/fullerene interfaces and at the electrodes (Figure 6). Further work on optimization of device structure of polymer **P1** is

expected to result in improved photovoltaic performance. Additionally, further investigation regarding the morphological features of pristine polymer **P1** and its corresponding blends with PCBM are currently under investigation. If polymer **P1** proves to form columnar morphology by casting from high boiling points solvents, a bilayer solar cell structure is expected to outperform the bulk heterojunction solar cells presented in this paper.

Conclusion

Novel semiconducting polymers containing benzodithiophene with phenylethynyl substituents containing more soluble longer decyl and hexadecyl alkyl chains have been synthesized. The HOMO and LUMO energy levels of the synthesized polymers with decyl and hexadecyl substituents were estimated from cyclic voltammetry and found to be similar, as expected on the basis of their structural similarity. TMAFM analysis of thin films of polymers deposited from chloroform indicates the formation of a granular morphology. The photovoltaic properties of polymers were investigated in bulk heterojunction solar cells with [6,6]-phenyl-C61-butyric acid methyl ester (PCBM). The benzodithiophene polymer with decyl phenylethynyl substituents showed better performance in solar cell devices. Solar cell devices obtained by slow evaporation of solvent generated a smoother surface and smaller phase aggregation features. The solar cell devices obtained by slow evaporation gave better power conversion efficiencies for 4-decyl and 4-hexadecyl phenylethynyl substituted benzodithiophene polymers.

Acknowledgment. Mihaela C. Stefan gratefully acknowledges financial support from UTD (start-up funds) and NSF (Career DMR-0956116). We gratefully acknowledge Dr. Anvar Zakhidov for giving us access to his solar cell fabrication lab.

Supporting Information Available: ^{1}H NMR spectra of monomers and polymers, phase and height TMAFM images of polymers, liquid and solid state UV−vis spectra of copolymers, fluorescence spectra, cyclic voltammograms of polymers. This material is available free of charge via the Internet at http://pubs.acs.org.

References and Notes

(1) Skotheim, T. A.; Reynolds, J. *Handbook of Conducting Polymers*, 3rd ed.; CRC Press: Boca Raton, FL, 2006.
(2) Bao, Z.; Locklin, J. *Organic Field-Effect Transistors*; CRC Press: Boca Raton, FL, 2007.
(3) Mullen, K.; Scherf, U. *Organic Light Emitting Devices: Synthesis, Properties and Applications*; Wiley-VCH: Weinheim, 2006.
(4) Brabec, C. J., Dyakonov, V., Parisi, J., Sariciftci, N. S., Eds.; *Organic Photovoltaics: Concepts and Realization*; Springer-Verlag: Heidelberg, 2003.
(5) Brabec, C. J.; Sariciftci, N. S.; Hummelen, J. C. *Adv. Funct. Mater.* **2001**, *11*, 15–26.
(6) Brabec, C.; Dyakonov, V.; Scherf, U. *Organic Photovoltaics; Materials, Device Physics, and Manufacturing Technologies*; Wiley-VCH: Weinheim, 2008.
(7) Sun, S.-S.; Dalton, L. R. *Introduction to Organic Electronic and Optoelectronic Materials and Devices*; CRC Press: Boca Raton, FL, 2008.
(8) Perepichka, I. F.; Perepichka, D. F. *Handbook of Thiophene-based Materials: Applications in Organic Electronics and Photonics*; Wiley: West Sussex, 2009.
(9) Hou, J.; Chen, H.-Y.; Zhang, S.; Li, G.; Yang, Y. *J. Am. Chem. Soc.* **2008**, *130*, 16144–16145.
(10) Liang, Y.; Wu, Y.; Feng, D.; Tsai, S.-T.; Son, H.-J.; Li, G.; Yu, L. *J. Am. Chem. Soc.* **2009**, *131*, 56–57.
(11) Pan, H.; Li, Y.; Wu, Y.; Liu, P.; Ong, B. S.; Zhu, S.; Xu, G. *Chem. Mater.* **2006**, *18*, 3237–3241.
(12) Pan, H.; Li, Y.; Wu, Y.; Liu, P.; Ong, B. S.; Zhu, S.; Xu, G. *J. Am. Chem. Soc.* **2007**, *129*, 4112–4113.
(13) Wang, Y.; Parkin, S. R.; Watson, M. D. *Org. Lett.* **2008**, *10*, 4421–4424.
(14) Hou, J.; Chen, H.-Y.; Zhang, S.; Chen, R. I.; Yang, Y.; Wu, Y.; Li, G. *J. Am. Chem. Soc.* **2009**, *131*, 15586–15587.
(15) Hou, J.; Chen, H.-Y.; Zhang, S.; Yang, Y. *J. Phys. Chem. C* **2009**, *113*, 21202–21207.
(16) Hou, J.; Park, M.-H.; Zhang, S.; Yao, Y.; Chen, L.-M.; Li, J.-H.; Yang, Y. *Macromolecules* **2008**, *41*, 6012–6018.
(17) Pan, H.; Wu, Y.; Li, Y.; Liu, P.; Ong, B. S.; Zhu, S.; Xu, G. *Adv. Funct. Mater.* **2007**, *17*, 3574–3579.
(18) Chen, J.; Shi, M.-M.; Hu, X.-L.; Wang, M.; Chen, H.-Z. *Polymer* **2010**, *51*, 2897–2902.
(19) Zhang, Y.; Hau, S. K.; Yip, H.-L.; Sun, Y.; Acton, O.; Jen, A. K. Y. *Chem. Mater.* **2010**, *22*, 2696–2698.
(20) Liang, Y.; Wu, Y.; Feng, D.; Tsai, S.-T.; Son, H.-J.; Li, G.; Yu, L. *J. Am. Chem. Soc.* **2009**, *131*, 56–57.
(21) Price, S. C.; Stuart, A. C.; You, W. *Macromolecules* **2010**, *43*, 4609–4612.
(22) Huo, L.; Hou, J.; Zhang, S.; Chen, H.-Y.; Yang, Y. *Angew. Chem., Int. Ed.* **2010**, *49*, 1500–1503.
(23) Zhang, G.; Fu, Y.; Zhang, Q.; Xie, Z. *Chem. Commun.* **2010**, *46*, 4997–4999.
(24) Beaujuge, P. M.; Subbiah, J.; Choudhury, K. R.; Ellinger, S.; McCarley, T. D.; So, F.; Reynolds, J. R. *Chem. Mater.* **2010**, *22*, 2093–2106.
(25) Zou, Y.; Najari, A.; Berrouard, P.; Beaupre, S.; Reda Aich, B.; Tao, Y.; Leclerc, M. *J. Am. Chem. Soc.* **2010**, *132*, 5330–5331.
(26) Liang, Y.; Yu, L. *Acc. Chem. Res.* **2010**, ASAP.
(27) Piliego, C.; Holcombe, T. W.; Douglas, J. D.; Woo, C. H.; Beaujuge, P. M.; Frechet, J. M. J. *J. Am. Chem. Soc.* **2010**, *132*, 7595–7597.
(28) Hou, J.; Huo, L.; He, C.; Yang, C.; Li, Y. *Macromolecules* **2006**, *39*, 594–603.
(29) Hundt, N.; Palaniappan, K.; Servello, J.; Dei, D. K.; Stefan, M. C.; Biewer, M. C. *Org. Lett.* **2009**, *11*, 4422–4425.
(30) Cox, E. G.; Cruickshank, D. W. J.; Smith, J. A. S. *Proc. R. Soc. London, Ser. A* **1958**, *247*, 1–21.
(31) Williams, J. H. *Acc. Chem. Res.* **1993**, *26*, 593–598.
(32) Li, H.; Powell, D. R.; Firman, T. K.; West, R. *Macromolecules* **1998**, *31*, 1093–1098.
(33) Beimling, P.; Kobmehl, G. *Chem. Ber.* **1986**, *119*, 3198–3203.
(34) Birckner, E.; Grummt, U.-W.; Göller, A. H.; Pautzsch, T.; Egbe, D. A. M.; Al-Higari, M.; Klemm, E. *J. Phys. Chem. A* **2001**, *105*, 10307–10315.
(35) Chu, Q.; Pang, Y. *Spectrochim. Acta, Part A* **2004**, *60*, 1459–1467.
(36) Brown, P. J.; Thomas, D. S.; Köhler, A.; Wilson, J. S.; Kim, J.-S.; Ramsdale, C. M.; Sirringhaus, H.; Friend, R. H. *Phys. Rev. B* **2003**, *67*, 064203/1–064203/16.
(37) Watts, B.; Belcher, W. J.; Thomsen, L.; Ade, H.; Dastoor, P. C. *Macromolecules* **2009**, *42*, 8392–8397.
(38) Burke, K. B.; Belcher; Thomsen, L.; Watts, B.; McNeill, C. R.; Ade, H.; Dastoor, P. C. *Macromolecules* **2009**, *42*, 3098–3103.
(39) Li, G.; Shrotriya, V.; Huang, J.; Yao, Y.; Moriarty, T.; Emery, K.; Yang, Y. *Nature Mater.* **2005**, *4*, 864–868.
(40) Yao, Y.; Hou, J.; Xu, Z.; Li, G.; Yang, Y. *Adv. Funct. Mater.* **2008**, *18*, 1783–1789.
(41) Scharber, M. C.; Mühlbacher, D.; Koppe, M.; Denk, P.; Waldauf, C.; Heeger, A. J.; Brabec, C. J. *Adv. Mater.* **2006**, *18*, 789–794.